

Effect of the fluid velocity change on the linear stability of plane Poiseuille flow

Zhao Haojie^{1,2}, Tang Hongtao^{1,2}, Cao Xiuming^{1,2}, Zhang Tingshuo^{1,2}, Chen Jiahui^{1,2}

¹Tianjin University of Science and Technology, Tianjin, 300222, China

²Tianjin Key Laboratory of Integrated Design and Online Monitoring of Light Industry and Food Engineering Machinery & Equipment, Tianjin, 300222, China

Keywords: Aerospace propulsion system; stability; area; laminar flow; coalescence

Abstract: The numerical simulation has been done for the linear stability of plane Poiseuille flow by varying the fluid velocity in the local flowing field. The analysis of the results showed that the influence of varying the fluid velocity on the linear stability bears some common characteristics. The relation curves between the unstable zone area encircled by the neutral curves and the different normal coordinates can be divided into four different functional regions, the approximately unchanged region of neutral curves, the region trending to stability, the region trending to instability, the obscure region trending to stability or instability. The susceptible region of stability change is made of the region trending to stability and the region trending to instability or unstable region. But that in which form the flowing field changes the unstable zone area encircled by the neutral curves depends on the forms of velocity changes. This study result will provide a fine platform for both the experimental study of the hydrodynamic stability and the further improvement of the coalescence theory.

The theory of flow stability was initially proposed to explain the transition of flow from laminar to turbulent flow, as the cause of the transition was attributed to the instability of laminar flow. The problem it studies is: in a flow that was originally laminar, if there is a disturbance for some reason, how will this disturbance evolve. If various disturbances eventually attenuate and the flow returns to its original laminar state, then the laminar motion is stable. On the contrary, if certain disturbances do not attenuate, the original laminar flow will either transform into another type of laminar flow, or transition to turbulence, then the laminar flow is unstable^[1]. The stability of flow is not limited to the transition from laminar to turbulent flow, and the formation of many complex flow fields is related to some unstable mechanism. The diversity of the world stems from its instability^[2].

Although linear stability theory cannot describe the entire process of transition, it cannot be applied to stages where nonlinear effects play an important role. But it can indicate which velocity profile is unstable, which frequencies have the fastest vibration growth, and indicate how to change the parameters controlling flow to delay transition^[3]. Saric's research results indicate that if most of the wings of a large transport aircraft can maintain laminar flow, it can save 25% of fuel^[4]. Thibert^[5] pointed out that frictional resistance generally accounts for 50% of the total resistance of subsonic transport aircraft, while laminar resistance is 90% less than turbulent resistance. Therefore, studying the theory of flow stability has important application background for the design of aerospace, ships,

vehicles, etc. Based on this, a deep understanding of the transition mechanism and control of the transition process of the boundary layer is a prerequisite for accurately calculating aerodynamics and heat conduction^[2].

Schmid^[6] demonstrated through analysis of the energy flow between Fourier harmonics that linear mechanisms do play a major role in providing energy for the growth of disturbances during transition. Reddy^[7] believes that the transition in Poiseuille flow also undergoes classical transition phenomena, namely first (T-S wave) instability and second instability. Luo Jisheng, Wang Xinjun, and others^[8] used a time model to directly simulate the "sudden change" process of incompressible channel flow from laminar to turbulent transition. They found that the change in the stability characteristics of the mean flow profile played a crucial role in the "sudden change" process, while the stability characteristics of the mean flow profile changed significantly after disturbance correction, manifested as a significant increase in the unstable region and amplification rate of linear stability, a significant increase in the unstable region surrounded by the neutral curve, and an increase in the linear growth rate, which means that more waves are easily and quickly excited, ultimately leading to the generation of turbulence. Afterwards, the author conducted direct numerical simulations of incompressible boundary layer turbulence and discovered similar mechanisms. It was also found that if the initial disturbance is not antisymmetric in the spanwise direction, the spanwise average flow is not zero, which has a significant impact on stability and indicates that the turbulence obtained from numerical simulation is not completely random^[9]. Huang Zhangfeng et al^[10] conducted direct numerical simulations of the boundary layer transition process on a supersonic flat plate with an incoming Mach number of 4.5 using a time model. The research shows that although the second mode T-S wave is more unstable in laminar flow, the first mode unstable wave plays a decisive role in the sudden change of laminar flow into turbulence. However, some semi empirical theories have led to satisfactory predictions of transition in two-dimensional and axisymmetric incompressible flows, with the more refined being the direct use of linear stability theory, which is also useful for quantitative research. Recent studies have shown that stability theory is also useful for studying coherent structures after transitions.

There are many factors that affect flow stability, such as Reynolds number, upstream turbulence intensity, wall roughness, volume force, heat conduction, etc. The suction and blowing in of the boundary layer also have an impact on the stability of the boundary layer flow. Generally speaking, suction increases the stability of the flow while blowing promotes the instability of the flow. There are also some factors that affect the stability of laminar flow, such as the compressibility of the fluid.

At present, in the engineering calculation of turbulence, in addition to predicting the place or time of transition, it is sometimes necessary to accurately simulate the transition process to make the connection between laminar and turbulent sections more in line with the actual situation and improve calculation accuracy, which is not easy. If we can find more regularity in the transition process, it will be helpful for solving the above problems. The change in flow stability before the transition breakdown process in this problem is the most common and urgent problem in engineering and technical problems.

In the past, research on the stability of flow (including numerical simulation and experimental methods) has mainly focused on the study of external factors on the stability of boundary layer flow, without studying the regularity of the impact of small details on flow stability. However, this is important for us because theoretical workers, experimental researchers, and engineering technicians urgently need some regularly analyzed knowledge as practical guidance. Therefore, this study is based on this consideration. This study includes two aspects: the impact of changes in symmetric and asymmetric velocities in planar Poiseuille flow on flow stability; The effect of changes in the average flow velocity profile on favorable coalescence conditions in a planar Poiseuille flow^[11,12]. This study will extend the theory of flow stability to the study of coalescence theory.

1. Methods of numerical simulation

1.1 Calculation method

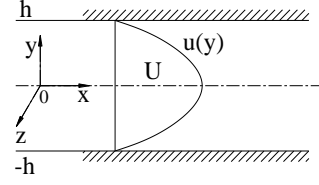


Fig. 1 Sketch of computational domain of plane Poiseuille flow

The computational domain of the planar Poiseuille flow studied in this article is shown in Figure 1. Dimensionalize the Navier Stokes equation and the continuity equation, using a reference length of half groove width h , a velocity U at the center (at $y=0$), and a pressure P using ρU^2 dimensionless. The Reynolds number Re is Uh/γ , where γ is the kinematic viscosity coefficient. The control equation and continuity equation are:

$$\begin{aligned} \frac{\partial u}{\partial t} + (u \cdot \nabla)u + \nabla p &= \frac{1}{Re} \nabla^2 u \\ \nabla \cdot u &= 0 \end{aligned} \quad (1)$$

Among them, u is the velocity vector, and its components are u , v , and w , which correspond to the x , y , and z -axis directions, respectively. ∇ is the gradient operator, and ∇^2 is the Laplace operator. The steady-state laminar solution for the two-dimensional flow of equation (1) is:

$$\begin{aligned} u_0 &= 1 - y^2, \quad v_0 = 0, \quad w_0 = 0, \\ p_0 &= -\frac{2}{Re}x + C \end{aligned} \quad (2)$$

Here, C is an arbitrary constant. To study whether the laminar flow is stable, it is necessary to assume that the flow deviates from the original flow. Therefore, velocity and pressure can be expressed as:

$$u = u_0 + u', \quad p = p_0 + p' \quad (3)$$

u' and p' represent the disturbance velocity and pressure. By substituting equation (3) into equation (1) and subtracting the equations satisfied by u_0 and p_0 , assuming that the perturbation momentum and its derivatives are small enough that their second-order terms can be omitted, a linearized perturbation equation can be obtained:

$$\begin{aligned} \frac{\partial u'}{\partial t} + (u_0 \cdot \nabla)u' + (u' \cdot \nabla)u_0 + \nabla p' &= \frac{1}{Re} \nabla^2 u' \\ \nabla \cdot u' &= 0 \end{aligned} \quad (4)$$

For convenience, the apostrophes on u' and p' will no longer be added. Due to the fact that the coefficients in equation (4) also do not include t , x , and z . When solving u and p in this way, the method of separating variables can be used and written as:

$$\begin{aligned} u &= \hat{u}(y)e^{i(\alpha x + \beta z - \omega t)} + c.c \\ p &= \hat{p}(y)e^{i(\alpha x + \beta z - \omega t)} + c.c \end{aligned} \quad (5)$$

Among them, *c.c* represents conjugate complex numbers. By substituting equation (5) into equation (4), we can obtain the equations that \hat{u} and \hat{p} satisfy. Written in component form:

$$L\hat{u} = \text{Re}(Du_0)\hat{v} + i\alpha \text{Re} \hat{p}, \quad L\hat{v} = \text{Re}(D\hat{p}),$$

$$L\hat{w} = i\beta \text{Re} \hat{p}, \quad i(\alpha\hat{u} + \beta\hat{w}) + D\hat{v} = 0 \quad (6)$$

$L = \{D^2 - (\alpha^2 + \beta^2) - i\text{Re}(\alpha u_0 - \omega)\}$. and \hat{u} should satisfy the boundary conditions: when $y = \pm 1$, $\hat{u} = 0$.

If the disturbance is also two-dimensional, i.e. $\hat{w} = 0$ and $\beta = 0$, then the above equation is transformed into a two-dimensional disturbance equation:

$$L\hat{u} = \text{Re}(Du_0)\hat{v} + i\alpha \text{Re} \hat{p}, \quad L\hat{v} = \text{Re}(D\hat{p}),$$

$$i\alpha\hat{u} + D\hat{v} = 0 \quad (7)$$

When the boundary condition is $y = \pm 1$, $\hat{v} = \pm 1$.

The equations of three-dimensional problems can be transformed into two-dimensional equations through the Squire transformation method. Therefore, the equation for a three-dimensional problem can be obtained in the same form as the equation for a two-dimensional problem. However, the three-dimensional problem still has an unknown function, which can be solved by solving another equation. It is obtained by multiplying β by the first equation of equation (6), subtracting α by the third equation:

$$L(\beta\hat{u} - \alpha\hat{w}) = \beta \text{Re}(Du_0)\hat{v} \quad (8)$$

By solving equation (6), u_1 and v_1 can be obtained. Because of $v_1 = \hat{v}$, the right end of equation (8) is known, and after solving $\beta\hat{u} - \alpha\hat{w}$, together with $u_1 = \beta\hat{u} + \alpha\hat{w}$, \hat{u} and \hat{w} can be solved separately.

Due to the homogeneous boundary conditions, there are generally only meaningless zero solutions. Only when the parameters α , β , Re , etc. in the equation satisfy certain relationships, can there be non-zero solutions. So, the linear stability problem is actually solving an eigenvalue problem.

The Orr-Sommerfeld equation satisfied by equation (7) is:

$$\{(D^2 - \alpha^2)^2 - i\alpha \text{Re}[(u_0 - \omega/\alpha)(D^2 - \alpha^2)] - D^2 u_0\} \cdot \hat{v} = 0 \quad (9)$$

When the boundary condition is $y = \pm 1$, $\hat{v} = D\hat{v} = 0$.

This article uses the finite difference method to discretize equation (6) in the y -direction. The finite difference format used is Malik's suggested compact difference format with two-point 4th order accuracy, which is:

$$\varphi_{j+1} - \varphi_j = \frac{\Delta y}{2} \left[\left(\frac{d\varphi}{dy} \right)_{j+1} + \left(\frac{d\varphi}{dy} \right)_j \right] - \frac{(\Delta y)^2}{12} \cdot \left[\left(\frac{d^2\varphi}{dy^2} \right)_{j+1} - \left(\frac{d^2\varphi}{dy^2} \right)_j \right] + O((\Delta y)^5) \quad (10)$$

Where φ is any sufficiently smooth function, it can be a vector function. The biggest feature of this format is that it only involves the functions and derivatives of two grid points, so it is also applicable to variable spacing. A more detailed calculation method can be found in reference [2].

By substituting the calculation result of equation (6) into the O-S equation, a complete system of equations for $\hat{v}_1, \hat{v}_2, \dots, \hat{v}_{N-1}$ can be obtained. The coefficient matrix of this system of equations is a banded diagonal matrix with a bandwidth of only 5. The Gaussian elimination method can be

used to calculate the value of its determinant. The usual method for solving eigenvalues is the müller method, which can be used to obtain new eigenvalues and their corresponding feature functions^[2].

1.2 Research Methods

There are two methods for studying flow stability in this article: blowing in method and suction out method. The so-called blowing in method refers to the way in which the fluid is blown in the direction of the flow direction to rapidly increase the velocity of the local flow field at that location, that is, the acceleration mode; The suction mode refers to the deceleration mode in which fluid is sucked out in the opposite direction of the flow direction to rapidly reduce the velocity of the local flow field at that location. Each way of changing speed can correspond to two forms of velocity distribution: symmetric and asymmetric. Due to the fact that the average flow profile of a planar Poiseuille flow is a symmetrical parabolic curve, the so-called symmetrical type refers to the distribution of the magnification and reduction of the speed that changes symmetrically on both sides of the axis of the standard average flow profile; On the contrary, it is asymmetric.

Due to the fact that the Navier Stokes equation and the continuity equation are dimensionless equations, the normal calculation domain is $[-1,1]$, the calculated grid points are 129, and the distribution of variable spacing grid points is $y_j = \cos(\pi \cdot j/N)$, $j = 0,1,2,\dots,N$, $N=128$. For the growth rate pattern, the velocity at a certain grid point is expressed as: $u_j = u_{j0} \cdot t$, where the increase and decrease multiples, $t = 0.1 \times i$, $i = 1,12,\dots,20$, $j = 0,1,2,\dots,N$, and u_{j0} represent the velocity at an unchanged grid point on the average flow profile; Similarly, the speed at a certain grid point in deceleration mode is the same as that in acceleration mode, except for $i = 9,8,\dots,0$.

In principle, the linear stability of flow field flow is characterized by the instantaneous maximum growth rate of the neutral stability curve. However, in order to enable theoretical researchers and engineering technicians to more intuitively observe the impact of velocity changes on flow stability, This article uses the area enclosed by the neutral curve to express the linear stability of instantaneous flow, which can basically reflect the main characteristics of statistical analysis of flow stability. Therefore, the area enclosed by the neutral stability curve is the integral of the closed curve in the $\beta - \alpha$ plane. For convenience in the following discussion, the area enclosed by the neutral stability curve is abbreviated as UZANC (The unstable zone area enclosed by the neutral curves), and the symbol S represents the area value.

2. Result analysis and discussion

From Figure 2(a), it can be seen that when $0.026 < y \leq 0.1572$, the area enclosed by a curve with a smaller value of the multiplication factor t can decrease rapidly, while the area enclosed by the curve with a large t value has little change in UZANC. However, the overall trend is that UZANC tends to be smaller than the area enclosed by the standard neutral curve. From the cross-sectional view at point $y = 0.0960$ in Figure 2(b), it is evident that the neutral curve disappears at $t=0.0\sim 0.34$, hence this region is referred to as the trending stable region; On the contrary, when $0.1572 < y \leq 0.3061$ is present, the area of a curve with a small increase or decrease factor t can rapidly increase, while a large t value corresponds to little change in UZANC. However, the overall trend is that UZANC tends to be larger than the area enclosed by the standard neutral curve. This situation can be clearly observed from the cross-sectional diagram at $y = 0.2270$ in Figure 2(c), and therefore, this area is called a trend unstable region. When $y > 0.3061$ is reached, UZANC is almost close to the area enclosed by the standard neutral curve, but the curves are all above the standard line, indicating that this region is an unstable

region with less significant changes. Moreover, it can be seen from the enlarged graph that as the t -value decreases, the flow tends to become more unstable. It is worth noting that when $0 \leq y \leq 0.026$ is present, the flow stability curve does not vary significantly with the t -value, and this region can be approximated as the neutral stability curve invariant region.

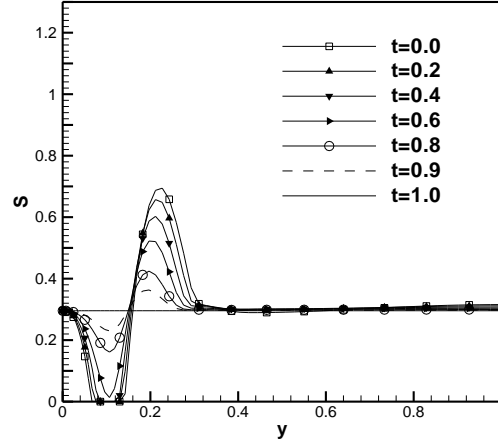


Fig. 2(a) Under the unsymmetrical and diminished fluid velocity, the curves of the UZANC at different normal position, y .

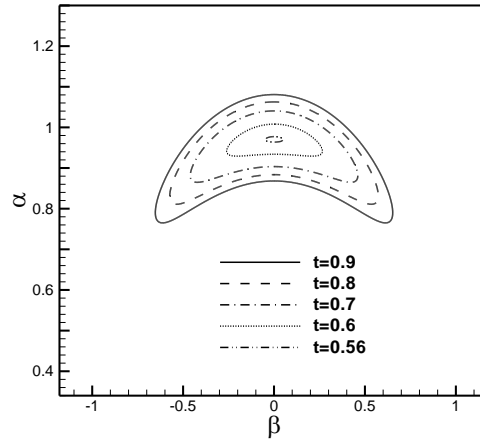


Fig. 2(b) Neutral curves of stability at $y = 0.0960$.

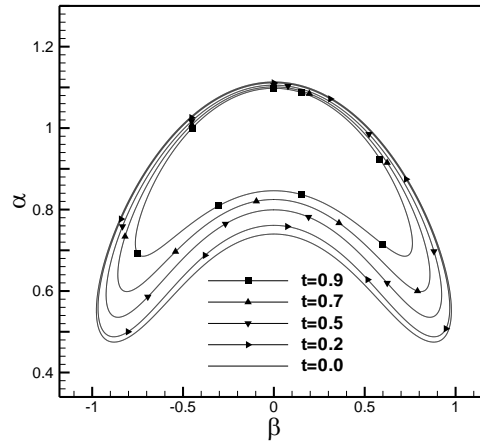


Fig. 2(c) Neutral curves of stability at $y = 0.2270$.

From Figure 3 (a), it can be seen that the area curve enclosed by the neutral stability curve is still similar to Figure 2 (a), that is, it undergoes significant changes with the amplification of velocity, and this change is more pronounced than Figure 2 (a). When $0 \leq y \leq 0.0206$, this region is the region where the neutral stability curve remains unchanged; It can be clearly seen from the cross-sectional view at point $y = 0.0960$ in Figure 3 (b) that UZANC reaches its maximum at $t=2.0$, and the peak in Figure 3 (a) corresponding to this point is greater than the peak in Figure 2 (a). Therefore, when $0.0206 < y \leq 0.1430$ is in an unstable region; When $0.1430 < y \leq 0.2690$ approaches the stable region of the neutral curve, that is, UZANC will significantly decrease or even disappear in this region as the increase or decrease factor t increases, as evidenced by the cross-sectional diagram at Figure 3 (c) $y = 0.1824$. Furthermore, from the cross-sectional view at $y = 0.1422$ in Figure 3 (d), it can be observed that the neutral stability curve splits into two symmetrical parts at $t=2.0$ as the increase or decrease factor t increases; When $y > 0.2690$ is reached, the area enclosed by the neutral curve is almost close to the standard line and below it, which is a stable region with less significant changes. And from the enlarged graph, it can be seen that as the value of t increases, the flow tends to become more stable. Furthermore, it can be seen that the regions in Figure 3 (a) are closer to the wall area compared to Figure 2 (a).

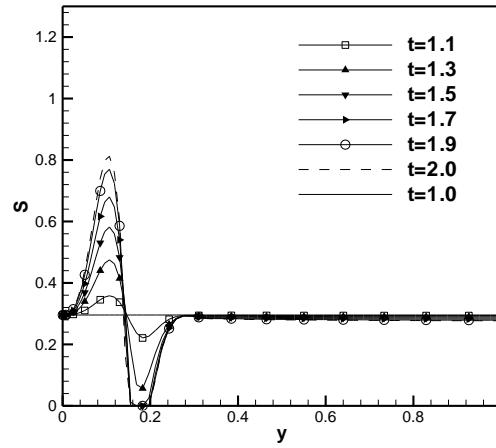


Fig. 3(a) Under the unsymmetrical and enlarged fluid velocity, the curves of the UZANC at different normal position, y .

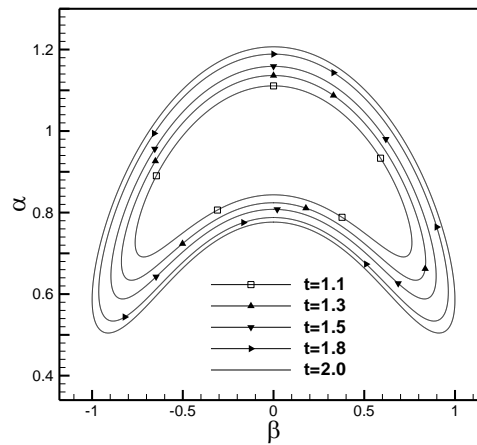


Fig. 3(b) Neutral curves of stability at $y = 0.0960$.

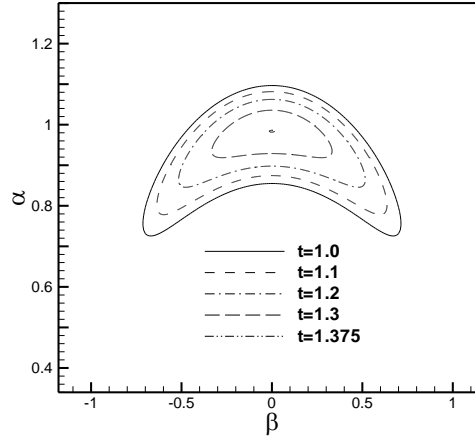


Fig. 3(c) Neutral curves of stability at $y = 0.1824$.

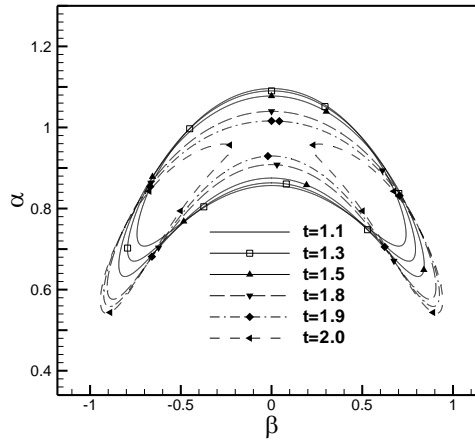


Fig. 3(d) Neutral curves of stability at $y = 0.1422$.

Figure 4(a) shows the relationship between the area of the neutral stability curve and the normal position of the flow field under symmetric reduction of flow velocity. From Figure 4(a), it can be seen that the pattern reflected by the curve in this figure is similar to that in Figure 3(a), except that due to the symmetrical reduction of the multiple of velocity, which is equivalent to an increase in the amplitude of velocity change. Thus, it leads to a rapid decrease or even disappearance to zero of UZANC in the approaching stable region ($0.0206 < y \leq 0.1541$) as the increment-decrement factor t decreases. (see the neutral stability curve at $y = 0.0960$ in Figure 4(b) for details), In the unstable region, the UZANC of ($0.1541 < y \leq 0.3135$) increases significantly as the increase or decrease factor t decreases (see the neutral stability curve at $y = 0.2270$ in Figure 4(c)). At point $y = 0.2270$, the maximum UZANC value is reached, which is more than three times the area enclosed by the standard neutral stability curve. When $y > 0.3135$, the flow field exhibits a tendency towards an unstable region with insignificant changes. On the other hand, compared with Figure 3(a), the normal position width of the two regions in Figure 4(a), namely the sum of the stable and unstable regions, has significantly widened. This result is clearly due to the symmetric change in velocity amplitude.

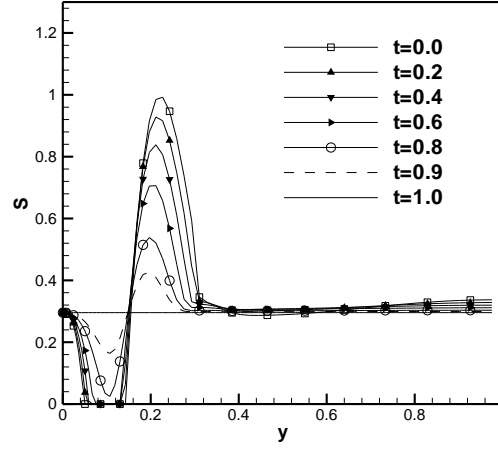


Fig. 4(a) Under the symmetrical and diminished fluid velocity, the curves of the UZANC at different normal position, y .

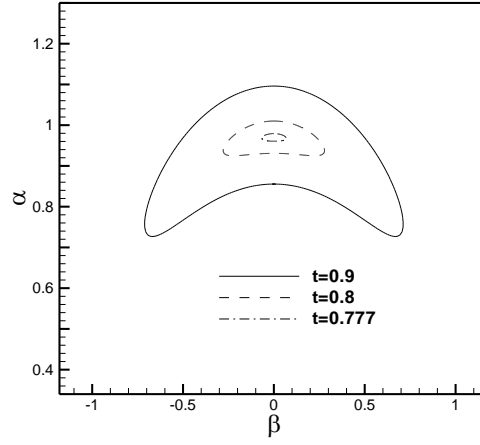


Fig. 4(b) Neutral curves of stability at $y = 0.0960$.

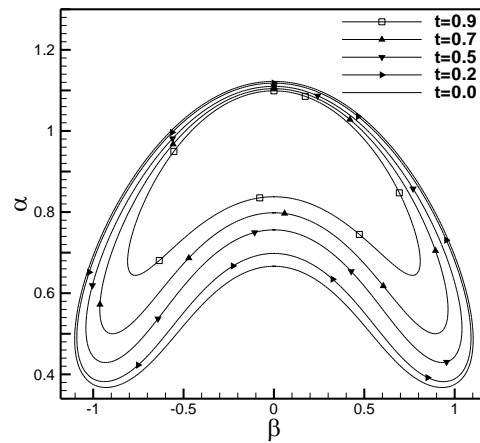


Fig. 4(c) Neutral curves of stability at $y = 0.2270$.

Figure 5(a) shows the relationship between the area of the neutral stability curve and the normal position of the flow field under symmetric amplification of flow velocity. Figure 5(a) shows similar characteristic patterns compared to Figure 3(a). Due to the symmetric amplification of flow velocity, UZANC exhibits rapid instability and disappearance in both the unstable region ($0.0206 < y \leq 0.1523$)

and stable region ($0.1523 < y \leq 0.2694$) under different amplification factors t , indicating that the stability of the flow field is sensitive to changes in flow velocity in both regions. These two situations can be clearly seen from the neutral stability curve at $y = 0.0960$ in Figure 5(b) and the neutral stability curve at $y = 0.1968$ in Figure 5(c). Furthermore, from the neutral stability curve at point $y = 0.1551$ in Figure 5(d), it can be observed that the area enclosed by the neutral stability curve rapidly decreases until it disappears when $t = 1.1 \sim 1.3$. However, when $t = 1.67$, the neutral stability curve reappears and exhibits two symmetrical branches on both sides. When $t = 1.7 \sim 2.0$, UZANC increases with the increase of t value. However, these neutral stability curves all exhibit symmetric branching forms. Therefore, it should be said that different values of t at the same point determine the different ways in which the neutral curve is presented. When $y > 0.2694$, the flow field exhibits a trend towards a stable region with no significant changes.

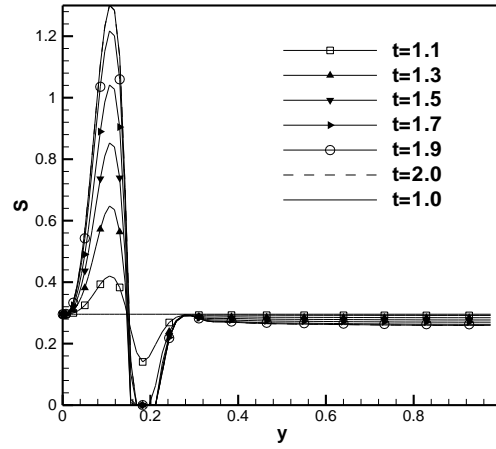


Fig. 5(a) Under the symmetrical and enlarged fluid velocity, the curves of the UZANC at different normal position, y .

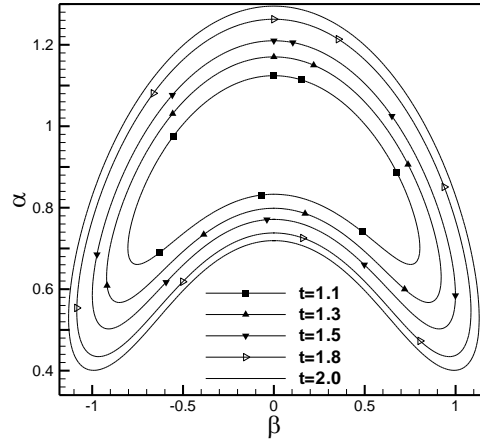


Fig. 5(b) Neutral curves of stability at $y = 0.0960$.

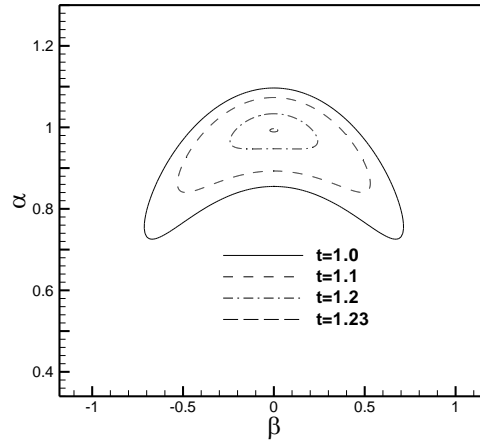


Fig. 5(c) Neutral curves of stability at $y = 0.1968$.

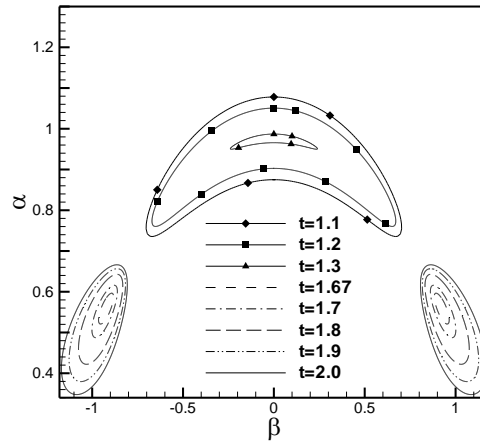


Fig. 5(d) Neutral curves of stability at $y = 0.1551$.

3. Conclusion

In summary, the following common characteristics of the impact of velocity changes on flow stability in planar Poiseuille flow can be summarized: ① The relationship curve between the area enclosed by the neutral stability curve and the normal position can be divided into four different functional regions. The neutral stability curve approximates the invariant region, the tending stable region, the tending unstable region, and the tending stable or unstable region with insignificant changes. Among them, stable or unstable regions together constitute sensitive areas for stability changes. As for the form in which the flow field will change, the area enclosed by the neutral stability curve depends on the way the velocity changes, such as symmetry, asymmetry, reduction, or amplification. ② The approximate invariant region of the neutral stability curve is of great significance for engineering technology research such as petrochemicals, especially for the agglomeration theory of stratified two-phase flow, as this region happens to be the most favorable agglomeration region obtained by the author and predecessors based on experiments. Therefore, the numerical calculation results of this article support the theory of the favorable agglomeration condition region obtained from known experiments. It is worth noting that the coalescence theory referred to in this article emphasizes the coalescence process between light phase small droplets and light phase liquid thin films in a layered two-phase flow in a planar Poiseuille flow^[11,12]. The greater the change in the average flow velocity profile, the greater the change in stability. Changes in the

average flow velocity profile can lead to diversity in flow stability, but to some extent, there are still patterns to follow.

Acknowledgement

This research was sponsored by the National Natural Science Foundation of China(52378254)and the Tianjin Higher Education Student Innovation Training Program Project under grants 202410057001.

References

- [1] Shi Xun-gang. *Turbulence*. Tianjin, Tianjin University Press, 1994, 1- 230 (in Chinese)
- [2] ZHOU Heng, ZHAO Geng-fu. *Hydrodynamic stability*. Beijing, National defence industry press, 2004, 1-255 (in Chinese).
- [3] CHEN Mao-zhang. *Fundamentals of viscous Fluid Dynamics*. Beijing, Higher Education Press, 2002, 1-512. (in Chinese).
- [4] Saric W S. *Physical description of boundary layer transition [J]. Experimental evidence*. In AGARD- CP-793, 1994.
- [5] Thibert J.J., Reneaux J., Schmitt V., *Onera activities in drag reduction[J]. Congr .Int. Counc. Aeron. Sci.(ICAS)1990,17:1053-1064.*
- [6] Schmid PJ, Henningson DS. *A new mechanism for rapid transition involving a pair of oblique waves[J]. Phys. Fluids,1992, 4:1986-89.*
- [7] Reddy SC, Schmid PJ, Baggett JS. *On stability of streamwise streaks and transition thresholds in plane channel flows[J]. J. Fluid Mech., 1998, 365: 269-303.*
- [8] Luo Jisheng, Wang Xinjun & Zhou Heng. *Inherent mechanism of breakdown in laminar-turbulent transition of plane channel flows[J]. Science in China, Ser. G, 2005, 48(2):228- 236.*
- [9] TANG Hongtao, LUO Jisheng, ZHOU Heng. *The mechanism of breakdown in laminar-turbulent transition of incompressible boundary layer on a flat plate[J]. Transactions of Tianjin University, 2007, 13(2):79-87.*
- [10] HUANG Zhangfeng, CAO Wei & Zhou Heng. *The mechanism of breakdown in laminar- turbulent transition of a supersonic boundary layer on a flat plate-temporal mode [J]. Science in China, Ser. G, 2005, 48(5):614-625.*
- [11] Walter Meon, Wolfgang Rommel and Eckhart Blass. *Plate separators for dispersed liquid-liquid systems: Hydrodynamic coalescence model[J]. Chemical Engineering Science, 2002, 46: 1437-1444.*
- [12] TANG Hong-tao, WU Jian-hua. *Investigation on the efficiency of plate separators for dispersed liquid-liquid system[J]. Transactions of Tianjin University, 2006, 12(5): 313-318.*